



Since January 2020 Elsevier has created a COVID-19 resource centre with free information in English and Mandarin on the novel coronavirus COVID-19. The COVID-19 resource centre is hosted on Elsevier Connect, the company's public news and information website.

Elsevier hereby grants permission to make all its COVID-19-related research that is available on the COVID-19 resource centre - including this research content - immediately available in PubMed Central and other publicly funded repositories, such as the WHO COVID database with rights for unrestricted research re-use and analyses in any form or by any means with acknowledgement of the original source. These permissions are granted for free by Elsevier for as long as the COVID-19 resource centre remains active.



# Synthesis, antimicrobial activity, density functional modelling and molecular docking with COVID-19 main protease studies of benzoxazole derivative: 2-(p-chloro-benzyl)-5-[3-(4-ethyl-1-piperazynl) propionamido]-benzoxazole



Celal Tuğrul Zeyrek<sup>a,\*</sup>, Özlem Temiz Arpacı<sup>b</sup>, Mustafa Arısoy<sup>b</sup>, Fatma Kaynak Onurdağ<sup>c</sup>

<sup>a</sup> Department of Academy and Publications, Turkish Energy, Nuclear and Mining Research Institution, TR-06100, Beşevler, Ankara, Turkey

<sup>b</sup> Department of Pharmaceutical Chemistry, Faculty of Pharmacy, Ankara University, TR-06100, Beşevler, Ankara, Turkey

<sup>c</sup> Department of Pharmaceutical Microbiology, Faculty of Pharmacy, Trakya University, TR-22030, Edirne, Turkey

## ARTICLE INFO

### Article history:

Received 11 November 2020

Revised 20 February 2021

Accepted 30 March 2021

Available online 8 April 2021

### Keywords:

Benzoxazoles

Density functional theory

Dpectroscopy

Molecular docking

Covid-19

## ABSTRACT

This study contains synthesis, antimicrobial activity, density functional modelling and molecular docking studies of benzoxazole derivative: 2-(p-chloro-benzyl)-5-[3-(4-ethyl-1-piperazynl) propionamido]-benzoxazole. The synthetic procedure of investigated compound is given in detail. The newly synthesized benzoxazole compound and standard drugs were evaluated for their antimicrobial activity against some Gram-positive, Gram-negative bacteria and fungus *C. albicans* and their drug-resistant isolates. The benzoxazole compound has been characterized by using <sup>1</sup>H-NMR, IR and MASS spectrometry and elemental analysis techniques. The molecular structure of the compound in the ground state has been modelling using density functional theory (DFT) with B3LYP/6-311++g(d,p) level. The molecular docking of 2-(p-chloro-benzyl)-5-[3-(4-ethyl-1-piperazynl) propionamido]-benzoxazole with COVID-19 main protease has been also performed by using optimized geometry and the experimentally determined dimensional structure of the main protease (M-pro) of COVID-19.

© 2021 Elsevier B.V. All rights reserved.

## 1. Introduction

During the last decades, a better comprehension of viral replication and disease states caused by viral infections have led to the development of newer antiviral agents with enhanced activity and better tolerability. However, because of limited efficacy of treatment and treatment-emergent antiviral resistance in infections there are needed urgently new compounds. Especially nowadays a great number of deaths and various public health problems are occurring throughout the globe because of COVID-19 which has been designated as SARS-CoV-2 around the globe [1,2]. The scientists around the world have been struggling to understand SARS-CoV-2 and investigate the pathophysiology of this disease to find out potential treatment and discover effective therapeutic drug candidate. Benzoxazole derivatives have acquired a lot of importance in the past few years because of their use in intermediates for new biological materials. Many known drugs are available

having benzoxazole as core active moiety like, nonsteroidal anti-inflammatory drug; flunoxapfen, benoxapfen, muscle relaxant-chloroxazone and an antibiotic; calcimycin. Benzoxazoles are important materials in medicinal chemistry due to their wide spectrum of different biological activities such as antimicrobial [3-5], anticancer [6], anti-inflammatory [7], antimicrobacterial [8], antihistaminic [9], antiparkinson [10], antiviral [11] and Rho-kinase inhibition [12]. Our research group has been intensively studying the synthesis of benzoxazoles and their molecular properties because of the importance of the benzoxazole derivatives [3-5, 8, 13,14]. Prompted by the above findings in the present study, we hereby report the synthesis, spectroscopic, antimicrobial activity, Density Functional Theory (DFT) calculations studies of the investigated new benzoxazole derivative. The molecular docking studies have become efficient tool for drug discovery and development. While traditional methods of drug discovery can take many years with high costs, the possible medications are investigated by using molecular docking studies in a short time and with very low costs. The experimentally determined dimensional structure of the main protease (M-pro) of COVID-19 which plays a pivotal role in medi-

\* Corresponding author.

E-mail address: [zeyrek@taek.gov.tr](mailto:zeyrek@taek.gov.tr) (C.T. Zeyrek).

ating viral replication and transcription are available in the Protein Data Bank (PDB) [15]. This protease represents a potential target for the inhibition of COVID-19 replication [15]. Therefore, we have also performed the molecular docking of 2-(p-chloro-benzyl)-5-[3-(4-ethyl-1-piperazynl) propionamido]-benzoxazole with COVID-19 main protease.

## 2. Materials and methods

### 2.1. Reagents and techniques

The analytical grade chemicals procured from Sigma-Aldrich Co. (Taufkirchen, Munich Germany) and Fisher Scientific (Pittsburgh, PA, USA) were used as such without further purification. Thin-layer chromatography on 0.3 mm silica gel (Merck) plates was performed for monitoring the progress of reaction, using chloroform and methanol as mobile phase in ratio of 3:1. Melting point was recorded on a Stuart Scientific SMP 1 (Bibby Scientific Limited, Stone, Staffordshire, UK) and are uncorrected. Shimadzu spectrometer was used for recording infrared spectrum. Varian Mercury 400 MHz NMR spectrometer was used for recording <sup>1</sup>H spectra in appropriate deuterated solvent and are expressed in parts per million (ppm) downfield from tetramethylsilane (internal standard). NMR data are given as multiplicity (s, singlet; d, doublet; t, triplet; m, multiplet) and number of protons. LECO 932 CHNS (St. Joseph, MI, USA) instrument C, H and N analyzer was utilized for the elemental analysis of the new synthesized compound. Mass spectra were obtained on Waters ZQ Micromass LC-MS spectrometer (Milford, MA, USA) using the ESI(+) method. Infrared absorption spectra of the investigated compound were obtained from Shimadzu IR Affinity-1 model FT-IR spectrometer and were reported in cm<sup>-1</sup> units. The FT-IR spectrum of the investigated compound (3) are given in Fig. S1 (Supplementary material).

### 2.2. Procedure for synthesis of benzoxazole derivatives

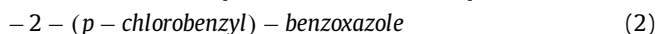
The method to synthesize the designed benzoxazole derivative is given in Fig. 1. Initially, 5-amino-2-(p-chlorobenzyl)-benzoxazole (1) was synthesized by the reaction of ortho aminophenol, p-chlorophenylacetic acid in polyphosphoric acid. 5-[3-chloropropanamido]-2-(p-chlorobenzyl)-benzoxazole (2) was synthesized by the reaction of 3-chloropropionylchloride with 5-amino-2-(p-chlorobenzyl)-benzoxazole in diethyl ether-water-sodium bicarbonate solution in ice-cooled condition. Finally, reaction of (2) with N-ethyl-piperazine gave the title compound with yield of %61 (3) (Fig. 1). Its melting point was 110-112°C. The molecular structures of the synthesized compound (3) were determined by IR (cm<sup>-1</sup>), <sup>1</sup>H/<sup>13</sup>C-NMR (DMSO-d<sub>6</sub>, 400 MHz, ppm), mass spectra and elemental analysis studies. The synthetic procedure of investigated compound (3) is given following step by step:

#### Step 1 : Synthesis of 2-(p-chlorobenzyl)



5-Amino-2-(p-chlorobenzyl)-benzoxazole was synthesized by heating (0.02 mol) 2,4-diaminophenol-hydrochloride with (0.02 mol) p-chlorophenyl acetic acid in 25 g polyphosphoric acid (PPA) and stirring for about 1 h at 160 °C. Then the residue was poured over ice, and the solution was neutralized with 10% NaOH. The resulting precipitate was filtered and was crystallized in ethanol [2].

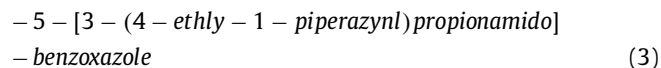
#### Step 2 : Synthesis of 5-[3-chloropropanamido]



Chloropropionyl chloride (0.02 mol) was added over a period of 1 h to a stirred, ice-cooled mixture of 5-amino-2-(p-chloro-

benzyl)-benzoxazole (0.02 mol) (1), sodium bicarbonate (0.02 mol), diethyl ether (40 ml), and water (20 ml). The mixture was stirred overnight. The precipitate formed was filtered off, washed with water, and dissolved in ethanol. Elemental analyses result was ± 0.04% of theoretical values for compounds (1), (2) and given as Supplementary material (Table S1).

#### Step 3 : Synthesis of 2-(p-chloro-benzyl)



Then, (0.002 mol) 5-(3-chloropropionamido)-2-(p-chlorobenzyl)-benzoxazole (2) was added to (0.002 mol) N-ethyl-piperazine 2 ml of triethylamine solution in 3 ml of N,N-dimethylformamide (DMF) and 2 ml of ethanol. The mixture was stirred at room temperature for 24 h. At the end of the reaction time, the mixture was poured over ice, an equal volume of 5% (w/v) of aqueous NaOH solution was added, and the mixture extracted with chloroform. The solvent was evaporated under reduced pressure, and the resulting crude product was purified by column chromatography using chloroform as mobile phase. Finally, the chloroform fractions were collected, the solvent evaporated, and crystallization was achieved by dissolving the residue in chloroform and adding petroleum ether. The crystalline material was dried in vacuo. The investigated compound 3 was prepared as original product. The structure of its was confirmed by spectral data and the analysis results agree with its of the proposed structure. Yield: %61, Melting Point: 110-112°C, <sup>1</sup>H-NMR (DMSO-d<sub>6</sub> δ ppm): 0.954-0.990 (3H, t, CH<sub>3</sub>CH<sub>2</sub>-), 2.256-2.516 (12H, m, piperazine -CH<sub>2</sub>, CH<sub>3</sub>CH<sub>2</sub>-, CH<sub>2</sub>-CO), 2.608-2.643 (2H, t, CH<sub>2</sub>-CH<sub>2</sub>CO), 4.334 (2H, s, benzyl CH<sub>2</sub>), 7.415-7.441 (5H, m, phenyl-H, benzoxazole H-6), 7.571-7.594 (1H, d, J<sub>o</sub>=9.2, benzoxazole H-7), 8.018-8.022 (1H, d, J<sub>m</sub>=1.6 benzoxazole H-4), 10.217 (1H, s). MS (m/z): 427(100, M+H) 429(33). C<sub>23</sub>H<sub>27</sub>ClN<sub>4</sub>O<sub>2</sub> Calculated C: 64.70 H: 6.37 N: 13.12, Observed C: 64.80 H: 6.55 N: 12.95

### 2.3. Screening for antimicrobial activities

Standard powders that were obtained Sigma, were used as standard antimicrobial agents. Isolates were; P. aeruginosa isolate [resistant to gentamycin], E. coli isolate [has Extended Spectrum Beta Lactamase (ESBL) enzyme], E. faecalis isolate [resistant to vancomycin (VRE)], and S. aureus isolate [resistant to methicillin (MRSA)]. Standard strains were; Escherichia coli ATCC 25922, Pseudomonas aeruginosa ATCC 27853, Staphylococcus aureus ATCC 29213, Enterococcus faecalis ATCC 29212 and Candida albicans ATCC 10231 standard strains and clinical isolates provided from Gazi University Hospital Microbiology Laboratory (Ankara, Turkey) were used in this research.

### 2.4. Calculation details

#### 2.4.1. DFT calculations

The molecular geometry of the compound is modelled by the Gauss-view visualization program [16] and the geometry optimization is performed by the Gaussian 09 software package program [17] for the DFT calculations with Becke's three parameters hybrid exchange-correlation functional (B3LYP) at 6-311++G(d,p) basis set [18]. MEP surface was evaluated by using B3LYP/6-311++G(d,p) method to investigate the reactive sites and to identify sites of intra- and intermolecular interactions of the compound. The total energy, frontier molecular orbitals energies, band gaps and chemical parameters such as total molecular dipole moments (μ), the absolute electro negativity (χ), the absolute hardness (η) and softness (σ) are calculated by the B3LYP/6-311++G(d,p).

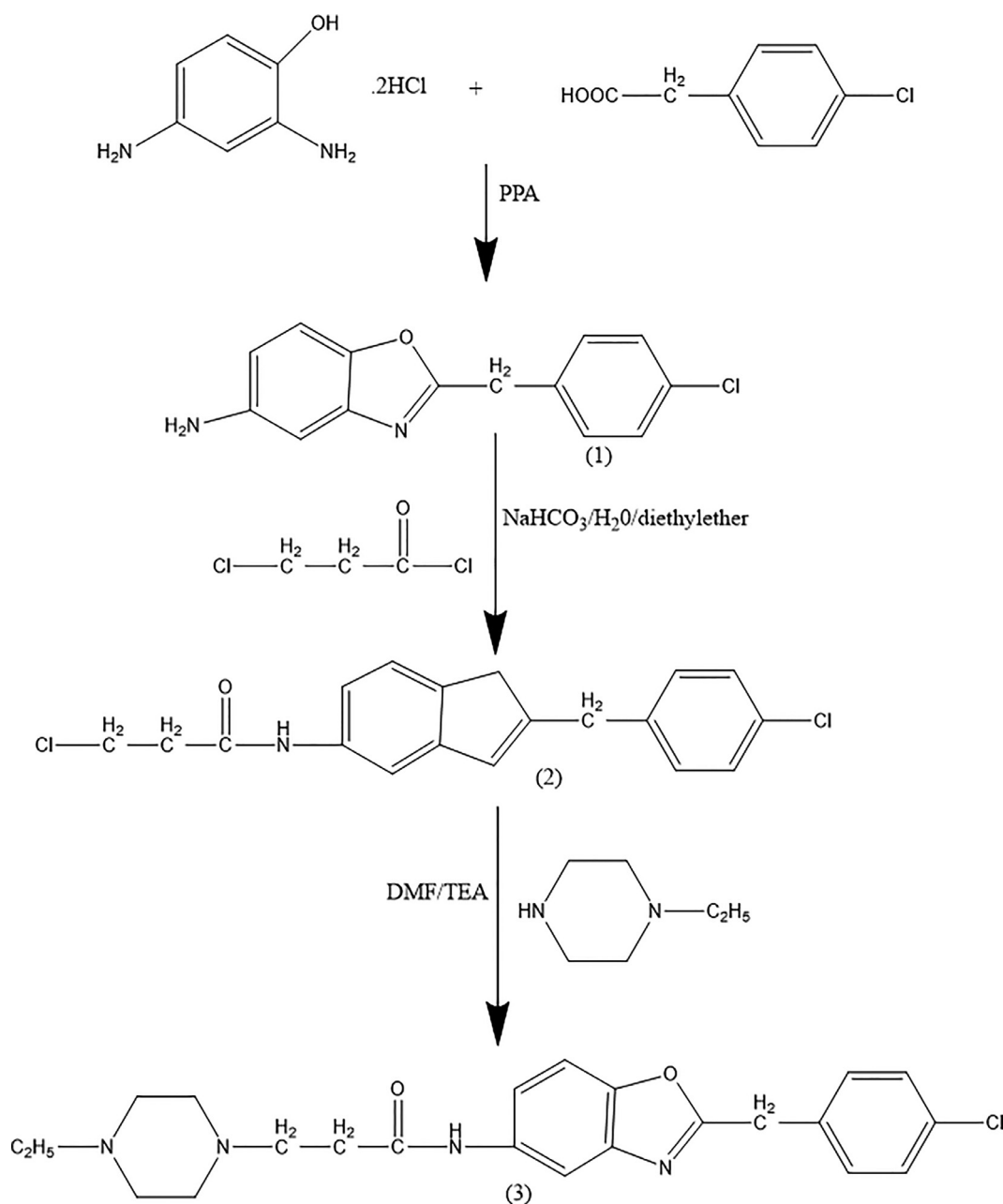


Fig. 1. The synthesize diagrams.

#### 2.4.2. Molecular docking

We have performed molecular docking calculations to examine the state of three dimensional structure of the main protease (M-pro) of COVID-19 settlement of investigated 2-(p-chlorobenzyl)-5-[3-(4-ethyl-1-piperazinyl) propionamido]-benzoxazole (**3**) compound. Thus to implement the molecular docking study, 3D molecular structure of the main protease (M-pro) in complex with an inhibitor N3 of COVID-19 virus which PDB ID number is 6LU7 was taken from the protein data bank [15]. The molecular geometry of the (**3**) was directly taken from the optimization results from output of Gaussian 09 software package program. The molecular docking simulations between inhibitor (**3**) and the SARS-CoV-2 main protease were performed using the AutoDock-Vina code, running 3-ways multithreading, Lamarckian Genetic Algorithm and the feasible region  $center_x = -26.283$ ,  $center_y = 12.599$ ,  $center_z = 58.965$ ,  $size_x = 50$ ,  $size_y = 60$ ,  $size_z = 60$ ,  $spacing = 1$  and  $exhaustiveness = 8$  [19]. All residues were removed and po-

lar hydrogens were added, producing favorable protonation states for molecular docking by using Discover Studio Visualizer 4.0 software [20]. The active site of the SARS-CoV-2 main protease was defined to include residues of active site within the grid size of  $50 \times 60 \times 60 \text{ \AA}$  for 6LU7. Between molecular docking executions were performed, the most favorable ones being represented by the lowest free-bond energy ( $\Delta G$ ) [21]. The other criteria is the Root Mean Square Deviation (RMSD) values which is lower than  $2 \text{ \AA}$  [22]. The interactions figures were drafted using Discover Studio Visualizer 4.0 software and PyMol [20, 23].

### 3. Results and discussions

#### 3.1. Spectroscopic studies

The presence of IR absorption respectively band at  $1682 \text{ cm}^{-1}$  and  $1618 \text{ cm}^{-1}$  in the spectral data of synthesized

derivative (1) corresponds to the group NH-C=O (amide I band and amide II band). Oxazole ring vibration of benzoxazole compounds shows band around 1476 cm<sup>-1</sup>. In case of halogen group Ar-Cl vibration appears at 760–799 cm<sup>-1</sup> (Fig. S1, Supplementary material). DMSO-d<sub>6</sub> was used for recording the <sup>1</sup>H-NMR spectra of benzoxazole derivative. In case of <sup>1</sup>H-NMR spectra the presence of multiplet signals between 7.42 and 7.44 ppm reflected the presence of phenyl and 6<sup>th</sup> position of benzoxazole ring protons in synthesized derivative. Also 7<sup>th</sup> position of benzoxazole ring proton and 4<sup>th</sup> position of benzoxazole ring proton appeared respectively at 7.571–7.594 ppm (1H, d, *J*<sub>o</sub>=9.2Hz) and, 8.018–8.022 (1H, d, *J*<sub>m</sub>=1.6 Hz). The compound showed singlet at 10.22 ppm because of the presence of NH of NH-C=O. The appearance of singlet at 4.33 ppm, is due to the existence of benzylic CH<sub>2</sub> group. Compound 3 showed triplet around 2.61–2.64 ppm and 0.95–0.99 ppm respectively due to existence of CH<sub>2</sub>-CH<sub>2</sub>CO group at CH<sub>2</sub> protons and CH<sub>3</sub> protons of ethyl group. Also compound (3) showed that multiplet at range of 2.26–2.52 ppm as 12 H due to presence of piperazine CH<sub>2</sub>, CH<sub>2</sub> protons of ethyl group and CH<sub>2</sub> protons of CH<sub>2</sub>-CO group. According to Mass spectral data, its M+H peak was observed that the spectral signals and proposed molecular structure of the prepared compound showed good agreement. Finally, elemental analyses result was ± 0.04% of theoretical values.

### 3.2. Optimized molecular structure

The molecular structure of 2-(p-chloro-benzyl)-5-[3-(4-ethyl-1-piperazynyl) propionamido]-benzoxazole (3) compound has been modelled by the Gauss-view visualization program [16] and optimized by the Gaussian 09 software package program [17]. The bond lengths, bond angles, and dihedral angles of the title compound were calculated by using density functional theory (DFT) with the functional B3LYP using the 6-311++G(d,p) basis set. The selected bond distances, bond angles and torsion angles are given in the Table 1. The optimized molecular geometry with atom label of the investigated compound is given in Fig. 2.

As an optimized geometry, whole of moieties is not nearly planar. The torsion angles for 2-(p-chloro-benzyl) ring Ph1 with the benzoxazole Ring3 are C19-C18-C17-C16= -113.59, C18-C17-C16-O2=74.40 and C18-C17-C16-N4=-104.23°. The propionamido group is tilted from the phenyl ring Ph2 which is evident from the torsion angles C11-C10-N3-C9= -175.37 and C8-C9-N3-C10=177.75°. The torsion angle N2-C7-C8-C9 value between with piperazynyl ring and propionamido group is -64.29°. The angles between 2-(p-chloro-benzyl) ring Ph1, benzoxazole Ring3 and the phenyl ring Ph2 are 76.75 and 76.67° respectively.

The bond distances, bond angles and torsion angles which are theoretically determined by DFT with the functional B3LYP using the 6-311++G(d,p) basis set in the investigated compound are good consistent with experimentally (X-ray structure analysis) corresponding values of similar benzoxazoles derivatives in the literature [13,14, 24].

### 3.6. Molecular electrostatic potential surface

The electrostatic potential is well suited for analyzing processes based on the “recognition” of one molecule by another, as in drug-receptor, and enzyme–substrate interactions, because it is through their potentials that the two species first “see” each other [25, 26]. To investigate the regions of the MEP for the title compound was composed by DFT calculation using the optimized geometry at the B3LYP/6-311++G(d,p). The MEP surface, electrophilic reactivity (negative regions: red and yellow colours) and nucleophilic reactivity (positive regions: blue colours) shown in Fig. 3. As can be seen from Fig. 3, the compound has three possible sites for

electrophilic attack. The O1, N1 and Cl1 atoms have negative region. The negative molecular electrostatic potential value for is the O1, N1 and Cl1 atoms 0.060, 0.041 and 0.016 a.u., respectively. The main regions for nucleophilic reactivity in the whole molecule is 2-(p-chloro-benzyl) ring Ph1, the propionamido group and the piperazynyl ring. These groups have positive region between 0.013–0.024 a.u.

### 3.7. HOMO-LUMO band gap and chemical parameters

The determining highest occupied molecular orbital (HOMO) and the lowest unoccupied molecular orbital (LUMO) are key to calculating chemical parameters and very important for chemical stability because of these orbitals play an important role in the electric properties and determine the way the molecule interacts with other species [27, 28]. In the other words, HOMO and LUMO are the main orbitals for the chemical reactions.

The HOMO represents the ability to donate an electron, whereas LUMO represents the ability to obtain an electron. Thus, the HOMO is directly related to the ionization potential (*IP*), while LUMO is directly related to the electron affinity (*EA*). According to the Koopman's theorem [29] for closed-shell molecules, *IP* and *EA* can be expressed as follows in terms of HOMO and LUMO energies:

$$IP = -E_{LUMO} \quad (5)$$

$$EA = -E_{HOMO} \quad (6)$$

If the values of *IP* and *EA* are predicted, HOMO-LUMO band gap and the global chemical reactivity descriptors of molecules such as chemical hardness (*η*), electronegativity (*χ*), softness (*σ*), chemical potential (*μ<sub>p</sub>*), and electrophilicity index (*ω*) as well as local reactivity can determine according to the Koopman's theorem.

The total molecular energies, HOMO and LUMO energies were predicted by the B3LYP/6-311++G(d,p) level for investigating. The values of total energy, HOMO-LUMO band gap and chemical parameters of the investigated compound were listed in Table 2. The frontier molecular orbital distributions and energy levels of the HOMO and LUMO which is mostly the π-antibonding type molecular orbitals of the title compound are shown in Fig. 4. Except for the propionamido group and the piperazynyl ring in the structure, the LUMO are mainly localized on the whole structure, whereas the HOMO is localized only on the 2-(p-chloro-benzyl) ring Ph1 with the benzoxazole Ring3 and phenyl ring Ph2, as seen from Fig. 4. The HOMO-LUMO gap was calculated to be 4.8795 eV. The large HOMO-LUMO band gap means a hard molecule whereas small band gap means a soft molecule. They are very important relation between HOMO-LUMO band gap and light-emitting properties of the benzoxazole derivatives [13].

### 3.8. Antimicrobial activity

Antimicrobial susceptibility testing was performed through CLSI M100-S18 and CLSI M27-A3 directions [12, 13]. Mueller Hinton Agar (MHA) (Merck), Mueller Hinton Broth (MHB) (Merck), Sabouraud Dextrose Agar (SDA) (Merck), Sabouraud Liquid Medium (SLM) (Merck) and RPMI-1640 medium (Sigma) with L-glutamine buffered pH 7 with 3-[N-morpholino]-propansulfonic acid (MOPS) (Sigma) were used for microbial cultures. Stock solutions of the test compounds were prepared in DMSO (Merck). Ampicillin was prepared in phosphate buffer solution and other antibiotic solutions were prepared in sterile distilled water according to the guideline of CLSI) M100-S25. Bacterial isolates were subcultured in Mueller Hinton Agar (MHA) plates and incubated over night at 37 °C and *C. albicans* was subcultured in Sabouraud Dextrose

**Table 1**

Optimized structural parameters using DFT/B3LYP with 6-311++G(d,p) basis set of the title compound in the ground state. Bond distances (Å) and angles (°).

Bond distances (Å)	B3LYP6-311++G(d,p)	Bond angles (°)	B3LYP6-311++G(d,p)	Selected torsion angles (°)	B3LYP6-311++G(d,p)
C1-C2	1.5276	C1-C2-N1	113.799	C1-C2-N1-C3	-164.005
C2-N1	1.4633	C2-N1-C3	111.392	C1-C2-N1-C6	70.446
N1-C3	1.4881	N1-C3-C4	111.305	N1-C6-C5-N2	-28.290
N1-C6	1.4582	C3-C4-N2	110.204	N1-C3-C4-N2	-30.675
C3-C4	1.5416	C4-N2-C5	110.685	N2-C7-C8-C9	-64.293
C4-N2	1.4621	N2-C5-C6	111.058	C3-C4-N2-C7	-165.825
N2-C5	1.4729	C5-C6-N1	109.830	C6-C5-N2-C7	-162.835
C5-C6	1.5406	C6-N1-C2	114.558	C4-N2-C7-C8	163.516
N2-C7	1.4661	C6-N1-C3	109.924	C6-N2-C7-C8	-69.044
C7-C8	1.5375	C4-N2-C7	113.525	C8-C9-N3-C10	177.749
C8-C9	1.5333	C5-N2-C7	113.382	C7-C8-C9-O1	-143.052
C9-O1	1.2218	N2-C7-C8	113.916	C9-N3-C10-C15	4.790
C9-N3	1.3695	C7-C8-C9	117.346	C9-N3-C10-C11	-175.371
N3-C10	1.4102	C8-C9-N3	114.315	N3-C10-C15-C14	179.627
C10-C11	1.4157	C9-N3-C10	128.882	N3-C10-C11-C12	179.449
C11-C12	1.3909	N3-C10-C11	115.888	C15-C14-N4-C16	179.749
C12-C13	1.3838	N3-C10-C15	123.265	C12-C13-O2-C16	179.984
C13-C14	1.3953	C10-C11-C12	122.100	N4-C14-C13-C12	179.960
C14-C15	1.3945	C11-C12-C13	115.960	O2-C13-C14-C15	179.702
C15-C10	1.3997	C12-C13-C14	123.073	C13-O2-C16-C17	-178.664
C13-O2	1.3753	C13-C14-C15	121.182	C14-N4-C16-C17	178.528
O2-C16	1.3756	C14-C15-C10	116.837	N4-C16-C17-C18	-104.230
C16-N4	1.2910	C15-C10-C11	120.847	O2-C16-C17-C18	74.397
N4-C14	1.3995	C12-C13-O2	129.219	C16-C-17-C18-C23	66.554
C16-C17	1.4929	C13-O2-C16	103.978	C16-C-17-C18-C19	-113.590
C17-C18	1.5216	O2-C16-N4	115.272	C19-C20-C21-C11	179.936
C18-C19	1.3955	C16-N4-C14	104.755	C23-C22-C21-C11	179.920
C19-C20	1.3942	N4-C14-C13	108.287		
C20-C21	1.3894	O2-C16-C17	116.838		
C21-C11	1.7602	N4-C16-C17	127.878		
C21-C22	1.3921	C16-C17-C18	113.060		
C22-C23	1.3915	C17-C18-C19	121.054		
C23-C18	1.3988	C18-C19-C20	121.125		
		C19-C20-C21	119.041		
		C20-C21-C11	119.491		
		C11-C21-C22	119.451		
		C20-C21-C22	121.058		
		C21-C22-C23	119.138		
		C22-C23-C18	121.014		
		C23-C18-C19	118.624		

**Table 2**

Calculated chemical parameters of the title compound at B3LYP/6-311++G(d,p) level.

Basis Set	B3LYP/6-311G++(d,p)
$E_{TOTAL}$ (Hartree)	-1722.7301
$E_{HOMO}$ (eV)	-5.9492
$E_{LUMO}$ (eV)	-1.0697
$\Delta E_{Gap}$ (eV)	4.8795
$I$ (eV)	5.9492
$A$ (eV)	1.0697
$\mu$ (Debye)	7.4052
$\eta$ (eV)	2.4398
$\chi$ (eV)	3.5095
$\sigma$ (eV)	0.4099
$\mu_p$ (eV)	-3.5095
$\omega$	15.0245

$E_{TOTAL}$ : Total energy

$E_{HOMO}$  and  $E_{LUMO}$ : Energy values of HOMO and LUMO

$\mu$ : Total molecular dipole moments,

$I$ : Ionization potential,

$A$ : Electron affinity,

$\eta$ : Absolute hardness,  $(I-A)/2$ ,

$\chi$ : Electronegativity,  $(I+A)/2$ ,

$\sigma$ : Softness,  $1/\eta$ ,

$\mu_p$ : Chemical potential,  $-(I+A)/2$

$\omega$ : Electrophilicity,  $\mu_p^2/2\eta$ .

<sup>a</sup>  $\Delta E_{Gap} = (E_{LUMO} - E_{HOMO})$ : gap of energy,

Agar (SDA) plates at 35 °C for 24-48 h. Pure colonies were transferred to MHB and SLM for bacteria and fungi, respectively. They were incubated in the appropriate conditions overnight. After incubation, the bacterial suspensions used for inoculation were prepared at 105 cfu/ml by diluting fresh cultures at MacFarland 0.5 density (108 cfu/ml). Yeast suspensions were also prepared according to McFarland 0.5 density and a working suspension was made by a 1:100 dilution followed by a 1:20 dilution of the stock suspension ( $2.5 \times 10^3$  CFU/ml). Susceptibility testing was performed with MHB for bacteria and RPMI-1640 medium with L-glutamine buffered pH 7 with 3-[N-morpholino]-propansulfonic acid (MOPS) for fungi. The solution of the newly synthesized compounds and standard drugs were prepared at 512, 256, 128, 64, 32, 16, 8, 4  $\mu$ g/mL and 16, 8, 4, 2, 1, 0.5, 0.25, 0.125, 0.06, 0.03, 0.015, 0.0078  $\mu$ g/mL concentrations, respectively by diluting the stock concentrations in a microdilution tray with a multichannel pipette. After dilution, a 10  $\mu$ l bacterial or fungal inoculum was added to each well of the microdilution trays. The trays were incubated at 37 °C for bacteria and 35 °C for fungi, in a humid chamber and MIC end-points were read after 24 h of incubation. The lowest concentration of the compound that completely inhibits macroscopic growth was determined and minimum inhibitory concentrations (MICs) were reported.

All organisms were tested in triplicate in each run of the experiments. Solvents, pure microorganisms and pure media were used as control wells. The data on the antimicrobial activity of the com-

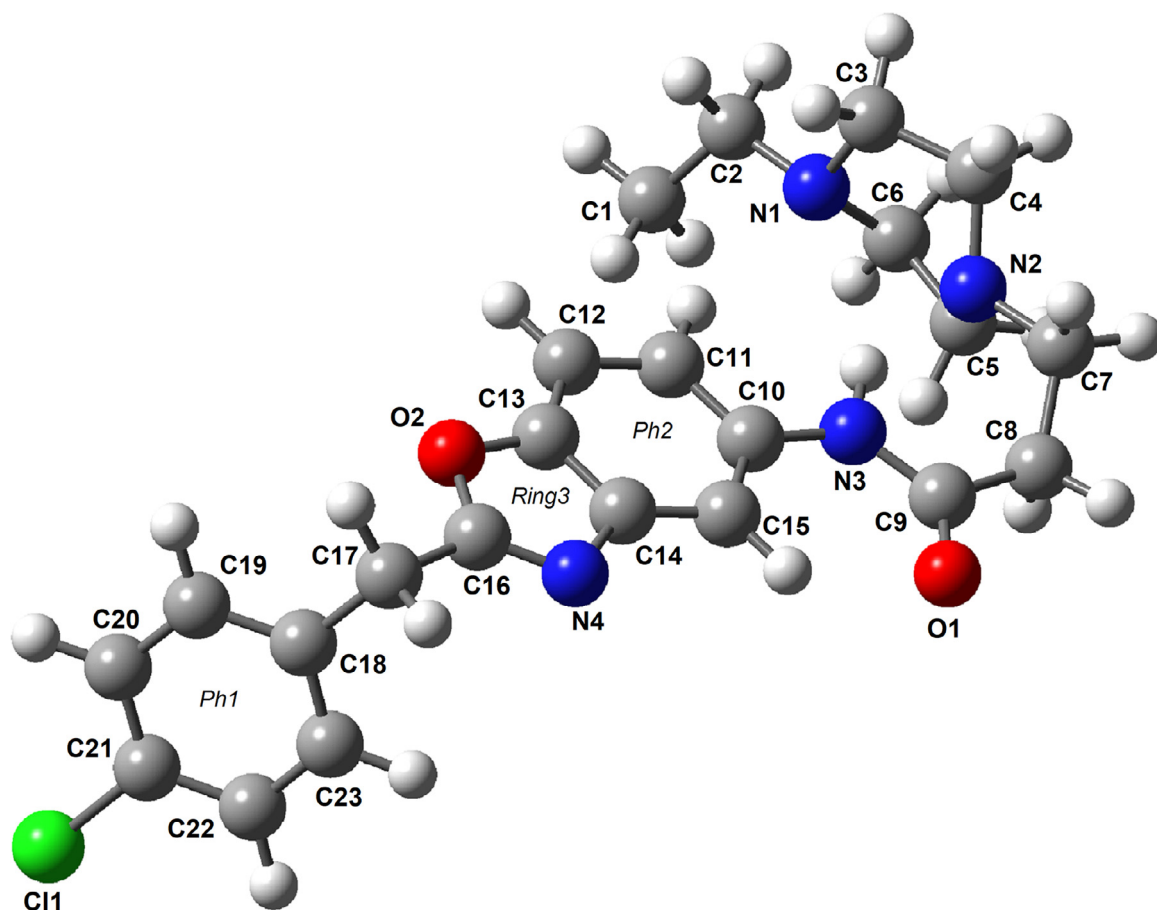


Fig. 2. Optimized geometry of investigated compound.

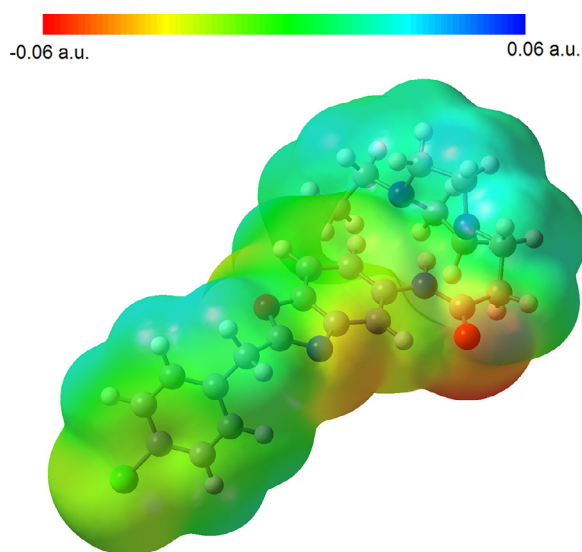


Fig. 3. Molecular electrostatic potential surface of the investigated compound.

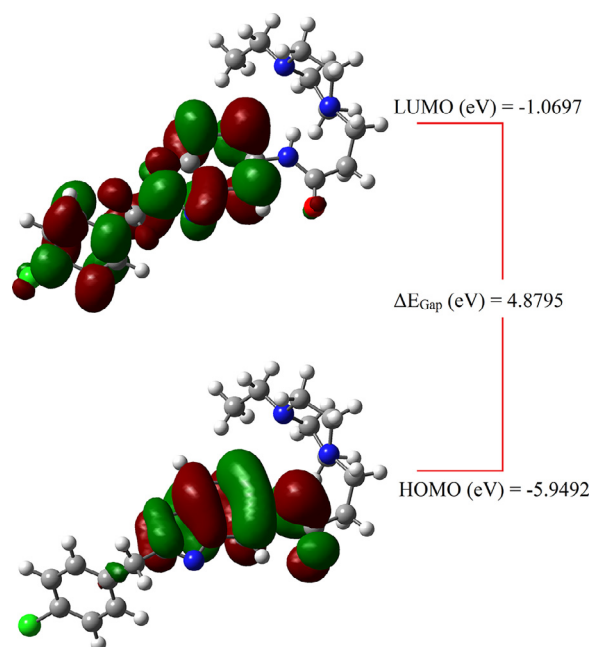


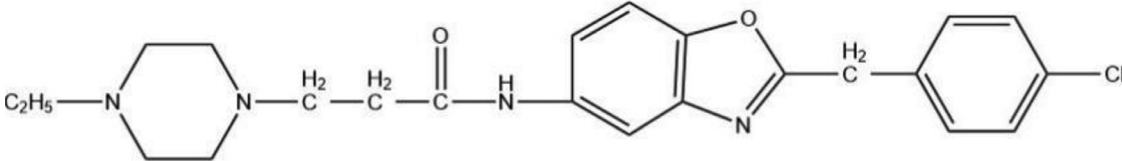
Fig. 4. Molecular orbital surfaces and energy levels given in parentheses for the HOMO and LUMO orbitals of the title compound computed at 6-311++G(d,p) level.

compound and the control drugs as MIC values ( $\mu\text{g/mL}$ ) are given in Table 3. Based on these data, the antimicrobial effect of this benzoxazole compound against various microorganisms has been detected in a broad spectrum.

When the benzoxazole ring system's chemical structure is investigated, it is thought that the nucleic acids are analog to the adenine and guanine bases in their structure and can show their

antimicrobial effects by inhibiting nucleic acid synthesis [30,31]. So that, studies on the benzoxazole derivatives have been increased in recent years [3, 32-34]. Antimicrobial activities of some benzox-

**Table 3**  
In vitro antibacterial and antifungal MIC values ( $\mu\text{g/mL}$ ) of the new compound (**3**) and reference antimicrobial drugs.



Comp. No	Gram-negative bacteria				Gram-positive bacteria				
	E.c.	E.c.*	Pa.	Pa.*	S.a.	S.a.*	E.f.	E.f.*	C.a.
<b>3</b>	64	64	64	64	128	256	64	32	128
<b>Vancomycin</b>	n.d	n.d	n.d	n.d	1	1	1	32	n.d
<b>Ampicillin</b>	2	128	n.d	n.d	2	64	2	2	n.d
<b>Ofloxacin</b>	<0,0625	64	8	64	0,25	0,25	1	4	n.d
<b>Gentamycin</b>	0.5	> 512	0.5	>512	0.125	32	4	32	n.d
<b>Amphotericin B</b>	n.d	n.d	n.d	n.d	n.d	n.d	n.d	n.d	0,25
<b>Fluconazole</b>	n.d	n.d	n.d	n.d	n.d	n.d	n.d	n.d	1

\* nd: not determined

**Table 4**  
Binding affinity of different poses of the investigated ligand (**3**) as predicted Autodock Vina.

Compound-inhibitor	Mode	Affinity Distance from best mode(kcal/mol)	RMSD	l.b.RMSD u.b.
<b>(3)- (6LU7)</b>	1	-6.1	0.000	0.000
	2	-6.0	22.045	25.624
	3	-6.0	27.555	31.601
	4	-6.0	26.621	30.749
	5	-5.9	27.359	31.497
	6	-5.9	29.657	33.283
	7	-5.9	22.296	26.690
	8	-5.8	22.722	24.648
	9	-5.8	28.833	33.034

**(3):** 2-(p-chloro-benzyl)-5-[3-(4-ethyl-1-piperazinyl) propionamido]-benzoxazole

azole derivatives obtained were observed equal or more effective than reference drugs. In previous studies, some derivatives containing p-(substituted)phenyl/benzyl at position 2 and 6-membered rings attached to the amide side chain at position 5 were synthesized, and promising results were obtained by examining their antimicrobial effects [35–38].

### 3.9. Molecular docking studies of 2-(p-chloro-benzyl)-5-[3-(4-ethyl-1-piperazinyl) propionamido]-benzoxazole with COVID-19 main protease

The study of molecules employing molecular docking has become increasingly relevant to predict bond modes to understanding of receptor-binder interactions. Benzoxazoles are important materials in medicinal chemistry due to especially their antimicrobial and antiviral inhibition [3–5, 11]. A new coronavirus which is named COVID-19 has spread worldwide and the World Health Organization (WHO) is declared a pandemic [1,2].

With the onset of the COVID-19 epidemic, studies have started on interactions of some Antiviral molecules with CoV-2 main protease with molecular docking simulations. Molecular modeling studies of this type are available on some quinoline and indole compounds with a long history as antiviral agents [39, 40]. Benzoxazoles, benzimidazoles and benzothiazoles are isosteres of indoles that indicate potent antiviral activity. A23187 is also known as Calcimycin that is a benzoxazole compound has potent anti-influenza activity [41, 42]. Based on this information, this study paved the way for further experimental evaluation of the benzoxazole molecule, which is thought to have potential antiviral effects against SARS-CoV-2.

To implement the molecular docking study, 3D molecular structure of the main protease (M-pro) in complex of COVID-19 virus (PDB ID: 6LU7). The generated bonding energy and RMSD values

as a result of molecular docking are given in Table 4. The docking protocol was tested by removing co-crystallized inhibitor from the main protease (M-pro) and then docking it at the same site as seen in Fig. 5a. Analysis of the molecular docking simulations showed that investigated new benzoxazole molecule are linked with relative binding energy value is -6.1 kcal/mol in site of the main protease (M-pro) in complex of COVID-19 virus. Energetically most favorable docked structures obtained from the rigid molecular docking of the compound 2-(p-chloro-benzyl)-5-[3-(4-ethyl-1-piperazinyl) propionamido]-benzoxazole with 6LU7 are shown in Fig. 5b. The interaction of 2-(p-chloro-benzyl)-5-[3-(4-ethyl-1-piperazinyl) propionamido]-benzoxazole with the protease showed a high affinity interaction in the main protease (M-pro) as the ligand fits inside the core pocket region of the protease (Fig. 5b). Analysis of interactions with 2-(p-chloro-benzyl)-5-[3-(4-ethyl-1-piperazinyl) propionamido]-benzoxazole showed that the molecular fitting simulation of the inhibitor (Fig. 6) resulted in the formation of four interactions type with the enzyme, one of the carbon hydrogen bonding between the C3 atom of the piperazinyl ring of investigated benzoxazole ligand with GLU166 (3.57 Å), a Pi-sigma bonding between the ph1 group of the ligand with THR25 (3.74 Å), two Pi-donor hydrogen bonding between the Rng3 and Ph2 groups of the benzoxazole ligand with CYS145 (3.73 and 4.01 Å). Some of the van der Waals interaction of the investigated new benzoxazole ligand with LEU27, MET49, HIS41, GLY143 and MET165 has been observed (Fig. 6). These results draw us to the conclusion that the investigated benzoxazole ligand might exhibit an inhibitor activity. But biological tests need to be done to validate the computational predictions. Docking calculations look for a suitable in site of the main protease (M-pro) in complex of COVID-19 virus and perform the interaction energy calculations using the topology of the site chosen beforehand.



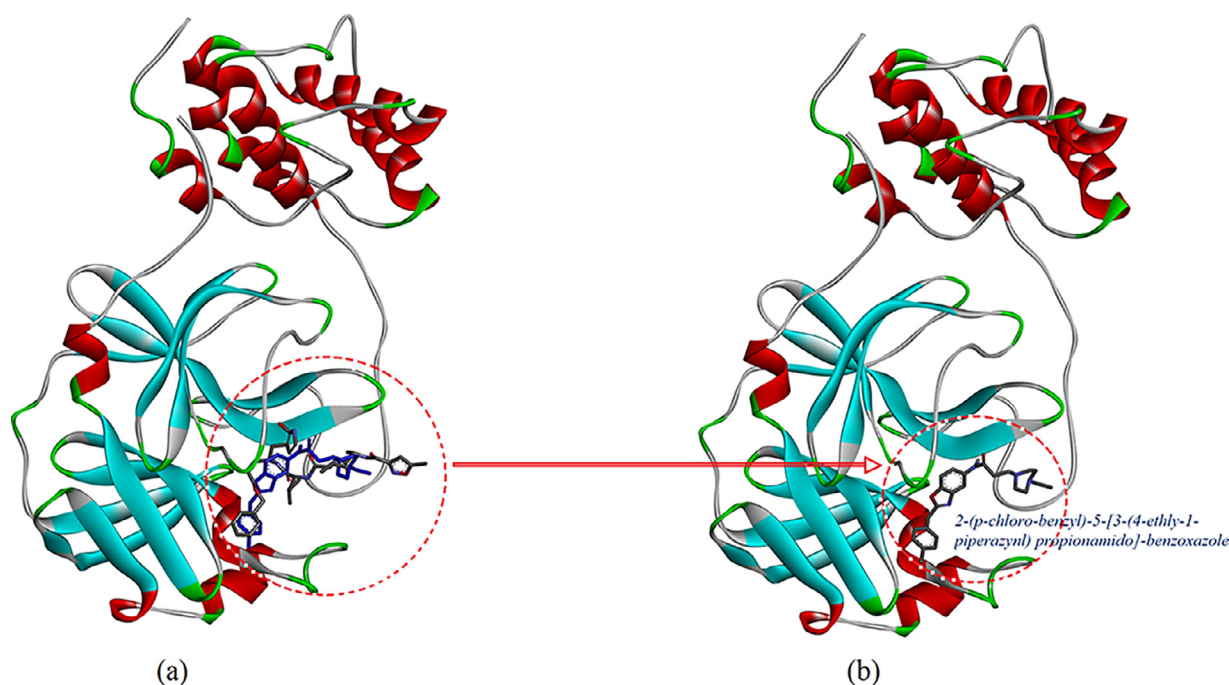


**Fig. 5.** (a) Co-crystallized molecule shown in grey color and the docked conformation of L (blue) as predicted by the Autodock Vina show very low RMSD value. (b) Representation of docking results of investigated a new benzoxazole compound embedded into the main protease (M-pro) in complex of COVID-19 virus (PDB ID: 6LU7). (For interpretation of the references to color in this figure legend, the reader is referred to web version of this article).

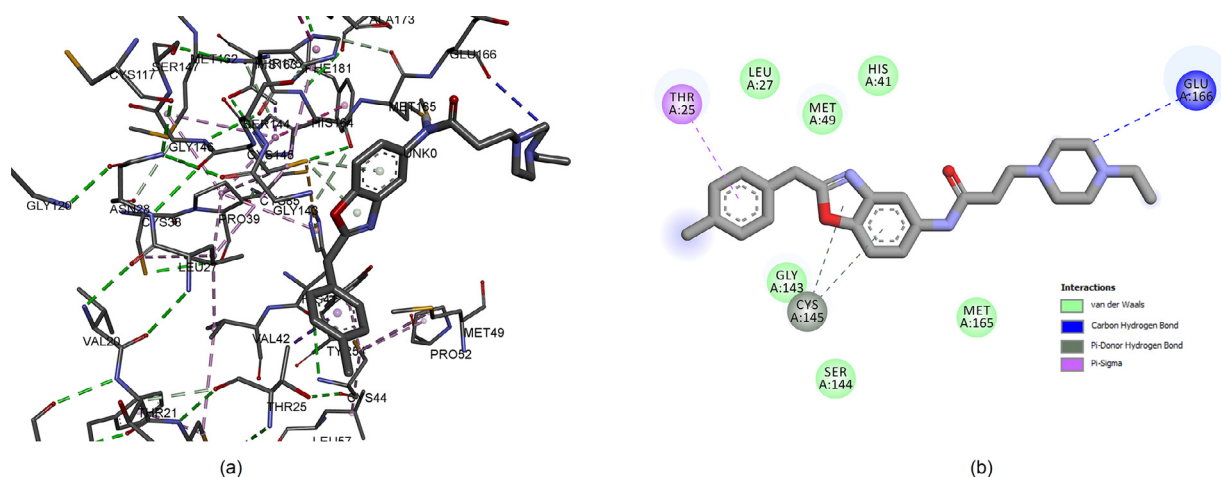


**Fig. 6.** (a) The ligand binds at the active site of the main protease (M-pro) in complex of COVID-19 virus (PDB ID: 6LU7). (b) 2-(p-chloro-benzyl)-5-[3-(4-ethyl-1-piperazynl) propionamido]-benzoxazole and 6LU7 interaction (2D).

#### 4. Conclusion

In this study, initially synthesis, spectroscopic (NMR, FTIR) and elemental analysis of a new benzoxazole compound titled 2-(p-chloro-benzyl)-5-[3-(4-ethyl-1-piperazynl) propionamido]-benzoxazole (compound 3) have been presented. Then, it was further evaluated for antibacterial, antifungal activity and it was observed that the compound 2-(p-chloro-benzyl)-5-[3-(4-ethyl-1-piperazynl) propionamido]-benzoxazole (compound 3) displayed the moderate activity against various microbial species in comparison to reference drugs. Also, The molecular structure of the compound 3 in the ground state has been molecular modelling using density functional theory (DFT) with B3LYP/6-311++g(d,p) level. The theoretical 3D-geometric parameters values of the new benzoxazole were quite agreement with the experimental values of the similar compound in literature. MEP surface was evaluated by

using B3LYP/6-311++G(d,p) method to predicted the reactive sites and to identify sites of intra- and intermolecular interactions of the compound. The O1, N1 and Cl1 atoms have negative region. The total energy, frontier molecular orbitals energies, band gaps and chemical parameters such as total molecular dipole moments ( $\mu$ ), the absolute electro negativity ( $\chi$ ), the absolute hardness ( $\eta$ ) and softness ( $\sigma$ ) are calculated by the B3LYP/6-311++G(d,p). The HOMO-LUMO gap was calculated to be 4.8795 eV. All organisms were tested in triplicate in each run of the experiments. Solvents, pure microorganisms and pure media were used as control wells. The data on the antimicrobial activity of the compound and the control drugs as MIC values ( $\mu\text{g/mL}$ ) are given in this study. The molecular docking of 2-(p-chloro-benzyl)-5-[3-(4-ethyl-1-piperazynl) propionamido]-benzoxazole with COVID-19 main protease has been also performed by using optimized geometry and the experimentally determined dimensional structure of the

main protease (M-pro) of COVID-19. The molecular fitting simulation of the inhibitor resulted in the formation of four interactions type with the enzyme; the carbon hydrogen bonding, Pi-sigma bonding, Pi-donor hydrogen bonding and van der Waals interaction. A virtual screening based on molecular docking emerges as an important tool for obtaining new antiviral molecules, where researchers can use this tool as a complementary approach so that the synthesis of new compounds or the repositioning of drugs can be assigned.

#### Author statement

**Celal Tuğrul Zeyrek:** Conceptualization, Methodology, Software, Molecular modelling, Visualization, Validation, Writing - original draft

**Özlem Temiz Arpacı:** Investigation, Resources, Writing- Original draft preparation, Synthesis and structure elucidation

**Mustafa Arısoy:** Investigation, Resources, Writing- Original draft preparation, Synthesis and structure elucidation

**Fatma Kaynak Onurdağ:** Investigation, Resources, Writing- Original draft preparation, Antimicrobial activity

#### Declaration of Competing Interest

The authors declare that they have no known competing financial interests or personal relationships that could have appeared to influence the work reported in this paper.

#### Supplementary materials

Supplementary material associated with this article can be found, in the online version, at [doi:10.1016/j.molstruc.2021.130413](https://doi.org/10.1016/j.molstruc.2021.130413).

#### References

- [1] P. Zhou, X-L. Yang, Wang X-G, B. Hu, L. Zhang, W. Zhang, H-R. Si, Y. Zhu, B. Li, C.L. Huang, H-D. Chen, J. Chen, Y. Luo, H. Guo, R-D. Jiang, M-Q. Liu, Y. Chen, X-R. Shen, X. Wang, X-S. Zheng, K. Zhao, Q-J. Chen, F. Deng, L-L Liu, B. Yan, F-X Zhan, Y-Y. Wang, G-F. Xiao, Z-L Shi, A pneumonia outbreak associated with a new coronavirus of probable bat origin, *Nature* 579 (2020) 270–273.
- [2] C. Wang, P.W. Horby, F.G. Hayden, G.F. Gao, A novel coronavirus outbreak of global health concern, *The Lancet* 395 (2020) 470–473.
- [3] M. Arısoy, O. Temiz-Arpaci, I. Yildiz, F. Kaynak-Onurdağ, E. Aki, I. Yalcin, U. Abbasoglu, Synthesis, antimicrobial activity and QSAR studies of 2,5-disubstituted benzoxazoles, *SAR and QSAR Environ. Res.* 19 5–6 (2008) 589–612.
- [4] O. Temiz-Arpaci, B.E. Cifcioglu-Goztepe, F. Kaynak-Onurdağ, S. Ozgen, F.S. Senol, I. Erdogan-Orhan, Synthesis and Different Biological Activities of Novel Benzoxazoles, *Acta Biologica Hungarica* 64 (2) (2013) 249–261.
- [5] M. Tasci, O. Temiz-Arpaci, F. Kaynak-Onurdağ, S. Okten, Synthesis and antimicrobial evaluation of 2-(p-tert-butylphenyl)benzoxazoles, *Ind. J. Chem.* 57B (2018) 385–389.
- [6] S. Aiello, G. Wells, E.L. Stone, H. Kadri, R. Bazzi, D.R. Bell, M.F.G. Stevens, C.S.T. Matthews, D. Bradshaw, A.D. Westwell, Synthesis and biological properties of benzothiazole, benzoxazole, and chromen-4-one analogues of the potent antitumor Agent 2-(3,4-dimethoxyphenyl)-5-fluorobenzothiazol, *J. Med. Chem.* 51 (16) (2008) 5135–5139.
- [7] S.M. Sondhi, N. Singh, A. Kumar, O. Lozach, L. Meijer, Synthesis, anti-inflammatory, analgesic and kinase (CDK-1, CDK-5 and GSK-3) inhibition activity evaluation of benzimidazole/benzoxazole derivatives and some Schiff's bases, *Bioorg. Med. Chem.* 14 (11) (2006) 3758–3765.
- [8] M. Arısoy, O. Temiz-Arpaci, F. Kaynak-Onurdağ, S. Ozgen, Synthesis and antimicrobial activity of novel benzoxazoles, *Z. Naturforsch* 67C (2012) 466–472.
- [9] Y. Katsura, Y. Inoue, S. Nishino, M. Tomoi, H. Itoh, H. Takasugi, Studies on antiulcer drugs. III. Synthesis and antiulcer activities of imidazo[1,2-a]pyridinylethylbenzoxazoles and related compounds. A novel class of histamine H2-receptor antagonists, *Chem. Pharm. Bull.* 40 (6) (1992) 1424–1438.
- [10] A. Benazzouz, T. Boraud, P. Dubedat, A. Boireau, J.M. Stutzmann, C. Gross, Riluzole prevents MPTP-induced parkinsonism in the rhesus monkey: a pilot study, *Eur. J. Pharmacol.* 284 (3) (1995) 299–307.
- [11] P. Smith, D.N. Ward, Heterocyclic benzoxazole compositions as inhibitors of hepatitis c virus, Publication Number WO/2011/047390 Publication Date 21.04.2011 International Application No, PCT/US2010/053085 International Filing Date 18 10 (2010).
- [12] E.H. Sessions, Y. Yin, T.D. Bannister, A. Weiser, E. Griffin, J. Pocas, M.D. Cameron, C. Ruiz, L. Lin, S.C. Schürer, T. Schröter, P. LoGrasso, Y. Feng, Benzimidazole- and benzoxazole-based inhibitors of Rho kinase, *Bioorg. Med. Chem. Lett.* 18 (24) (2008) 6390–6393.
- [13] C.T. Zeyrek, H. Unver, O. Temiz- Arpacı, K. Polat, N.O. İskeleli, M. Yildiz, Experimental and theoretical characterization of the 2-(4-bromobenzyl)-5-ethylsulphonyl-1,3- benzoxazole, *J. Mol. Struct.* 1081 (2015) 22–37.
- [14] C.T. Zeyrek, B. Boyacioglu, O. Temiz-Arpaci, H. Unver, A. Elmali, Spectroscopic, quantum mechanical and molecular docking studies of a new benzoxazole compound with an oxidoreductase enzyme and DNA, *J. Mol. Struct.* 1136 (2017) 112–126.
- [15] Z. Jin, X. Du, Y. Xu, Y. Deng, M. Liu, Y. Zhao, B. Zhang, X. Li, L. Zhang, C. Peng, Y. Duan, J. Yu, L. Wang, K. Yang, F. Liu, R. Jiang, X. Yang, T. You, X. Liu, X. Yang, F. Bai, H. Liu, X. Liu, L.W. Guddat, W. Xu, G. Xiao, C. Qin, Z. Shi, H. Jiang, Z. Rao, H. Yang, Structure of Mpro from SARS-CoV-2 and discovery of its inhibitors, *Nature* 582 (2020) 289–293.
- [16] R. Dennington, T. Keith, J. Millam, GaussView, Version 5, Semichem, Inc., Shawnee Mission, KS, 2009.
- [17] M.J. Frisch, G.W. Trucks, H.B. Schlegel, G.E. Scuseria, M.A. Robb, J.R. Cheeseman, G. Scalmani, V. Barone, B. Mennucci, G.A. Petersson, H. Nakatsuji, M. Caricato, X. Li, H.P. Hratchian, A.F. Izmaylov, J. Bloino, G. Zheng, J.L. Sonnenberg, M. Hada, M. Ehara, K. Toyota, R. Fukuda, J. Hasegawa, M. Ishida, T. Nakajima, Y. Honda, O. Kitao, H. Nakai, T. Vreven, J.A. Montgomery, J.E. P. Jr, F. Ogliaro, M. Bearpark, J.J. Heyd, E. Brothers, K.N. Kudin, V.N. Staroverov, R. Kobayashi, J. Normand, K. Raghavachari, A. Rendell, J.C. Burant, S.S. Iyengar, J. Tomasi, M. Cossi, N. Rega, J.M. Millam, M. Klene, J.E. Knox, J.B. Cross, V. Bakken, C. Adamo, J. Jaramillo, R. Gomperts, R.E. Stratmann, O. Yazyev, A.J. Austin, R. Cammi, C. Pomelli, J.W. Ochterski, R.L. Martin, K. Morokuma, V.G. Zakrzewski, G.A. Voth, P. Salvador, J.J. Dannenberg, S. Dapprich, A.D. Daniels, eO. Farkas, J.B. Foresman, J.V. Ortiz, J. Cioslowski, D.J. Fox, Gaussian 09, Revision D.01, Gaussian, Inc., Wallingford CT, 2009.
- [18] G.A. Petersson, A. Bennett, T.G. Tensfeldt, M.A. Allaham, W.A. Shirley, J. Mantzaris, A complete basis set model chemistry .1. The total energies of closed-shell atoms and hydrides of the 1st-row elements, *J. Chem. Phys.* 89 (4) (1988) 2193–2218.
- [19] O. Trott, A.J. Olson, Software news and update autodock vina: improving the speed and accuracy of docking with a new scoring function, efficient optimization, and multithreading, *J. Comput. Chem.* 31 (2) (2010) 455–461.
- [20] Accelrys Software Inc Discovery Studio Modelling Environment, Accelrys Software Inc, SanDiego, 2013 Relaser 4.0.
- [21] A.B. Gurung, M.A. Ali, A. Bhattacharjee, M. Abul Farah, F. Al-Hemaid, F.M. Abou-Tarboush, K.M. Al-Anazi, F.S.M. Al-Anazi, J. Lee, Molecular docking of the anticancer bioactive compound procazide with macromolecules involved in the cell cycle and DNA replication, *Genet. Mol. Res.* (2016), doi:10.4238/gmr.15027829.
- [22] B. Kramer, M. Rarey, T. Lengauer, Evaluation of the FLEXX Incremental Construction Algorithm for Protein-Ligand Docking, *Proteins* 37 (2) (1999) 228–241.
- [23] W.L. DeLano, The PyMOL Molecular Graphics System, San Carlos, CA, USA, 2016.
- [24] M. Sivakumar, K.Saravanan K. Rajavelu, P. Rajakumar, S. Aravindhan, Chemical Data Collections Synthesis, structural exploration and Hirshfeld surface analysis of a novel bioactive heterocycle: (4-(6-Fluorobenzod[isoxazol-3-yl] piperidin-1-yl)(morpholino)methanone, *Chemical Data Collections* 15–16 (2018) 161–169.
- [25] E. Scrocco, J. Tomasi, *Topics in Current Chem.* 7, Springer Berlin, 1973.
- [26] I. Fleming, in: *Frontier Orbitals and Organic Chemical Reactions*, John Wiley & Sons, New York, 1976, p. 182.
- [27] M. Govindarajan, S. Periandy, K. Carthigayen, *Spectrochim. Acta A*, FT-IR and FT-Raman spectra, thermo dynamical behavior, HOMO and LUMO, UV, NLO properties, computed frequency estimation analysis and electronic structure calculations on  $\alpha$ -bromotoluene, *Spectrochim. Acta Part A Mol. Biomol. Spectros.* 97 (2012) 411–422.
- [28] C. Ravikumar, I.H. Joe, V.S. Jayakumar, Charge transfer interactions and nonlinear optical properties of push-pull chromophore benzaldehyde phenylhydrazonone: A vibrational approach, *Chem. Phys. Lett.* 460 (2008) 552–558.
- [29] T. Koopmans, Über die Zuordnung von Wellenfunktionen und Eigenwerten zu den Einzelnen Elektronen Eines Atoms, *Physica* 1 (1933) 104–113.
- [30] S.M. Rida, F.A. Ashour, S.A. El-Hawash, M.M. El Semaary, M.H. Badr, M.A. Shalaby, Synthesis of some novel benzoxazole derivatives as anticancer, anti-HIV-1 and antimicrobial agents, *Eur. J. Med. Chem.* 40 (2005) 949–959.
- [31] L. Oehlers, C.L. Mazzitelli, J.S. Brodbelt, M. Rodriguez, S. Kerwin, Evaluation of complexes of DNA duplexes and novel benzoxazoles or benzimidazoles by electrospray ionization mass spectrometry, *J. Am. Soc. Mass Spectrom.* 15 (2004) 1593–1603.
- [32] T. Ertan, I. Yildiz, B. Tekiner-Gulbas, K. Bolelli, O. Temiz-Arpaci, S. Ozkan, F. Kaynak, I. Yalcin, E. Aki, Synthesis, biological evaluation and 2D-QSAR analysis of benzoxazoles as antimicrobial agents, *Eur. J. Med. Chem.* 44 (2009) 501–510.
- [33] B. Tekiner-Gulbas, O. Temiz-Arpaci, I. Yildiz, N. Altanlar, Synthesis and in vitro antimicrobial activity of new 2-[p-substituted-benzyl]-5-[substituted-carbonylamino]benzoxazoles, *Eur. J. Med. Chem.* 42 (2007) 1293–1299.
- [34] J.-i. Kuroyanagi, K. Kanai, T. Horiuchi, H. Takeshita, S. Kobayashi, I. Achiwa, K. Yoshida, K. Nakamura, K. Kawakami, Structure-activity relationships of

- 1,3-benzoxazole-4-carbonitriles as novel antifungal agents with potent in vivo efficacy, *Chem. Pharm. Bull.* 59 (2011) 341.
- [35] Ö. Temiz-Arpacı, A. Ozdemir, İ. Yalçın, İ. Yıldız, E. Akı-Şener, N. Altanlar, Synthesis and Antimicrobial Activity of Some 5-[2-(Morpholin-4-yl)acetamido] and/or 5-[2-(4-Substituted piperazin-1-yl)acetamido]-2-(p-substituted phenyl)benzoxazoles, *Arch. Pharm. Chem. Life Sci.* 338 (2005) 105–111.
- [36] Ö. Temiz-Arpacı, İ. Yıldız, S. Özkan, F. Kaynak, E. Akı-Şener, İ. Yalçın, Synthesis and biological activity of some new benzoxazoles, *Eur. J. Med. Chem.* 43 (2008) 1423–1431.
- [37] M. Arısoy, O. Temiz-Arpacı, F. Kaynak-Onurdag, S. Ozgen, Synthesis and antimicrobial evaluation of 2-(p-substituted phenyl)-5-[(4-substituted piperazin-1-yl)acetamido]-benzoxazoles, *Z. Naturforsch C J. Biosci.* 69 (2014) 368–374.
- [38] M. Arısoy, O. Temiz-Arpacı, F. Kaynak-Onurdag, S. Ozgen, Synthesis of some piperazinobenzoxazole derivatives and their antimicrobial properties, *Indian J. Chem. B.* 55 (2016) 240–247.
- [39] I.Celik, A.Onay-Besikci, G.Ayhan-Kilcigi, Approach to the mechanism of action of hydroxychloroquine on SARS-CoV-2: a molecular docking study, (2020) 1–13.
- [40] A. Llanes, H. Cruz, V.D. Nguyen, O.V. Larionov, P.L. Fernández, A computational approach to explore the interaction of semisynthetic nitrogenous heterocyclic compounds with the SARS-CoV-2 main protease, *Biomolecules* 11 (2021) 18–31.
- [41] V. Francesconi, E. Cichero, S. Schenone, L. Naesens, M. Tonelli, Synthesis and biological evaluation of novel (thio)semicarbazone-based benzimidazoles as antiviral agents against human respiratory viruses, *Molecules* 25 (7) (2020) 1487–1508.
- [42] S. Jantaratrirat, C. Boonarkart, K. Ruangrun, O. Suptawiwat, P. Auewarakul, Microparticle release from cell lines and its anti-influenza activity, *Viral Immunol.* 31 (6) (2018) 447–456.